

# Electrochemical Formation of Contacts between Platinum or Gold Electrodes with the Organic Charge-Transfer Salts Tetrathiafulvalenium Bromide (TTFBr<sub>x</sub>, $x = 0.74–0.79$ ) or Bis(tetramethyltetraselenafulvalenium) Perchlorate ((TMTSF)<sub>2</sub>ClO<sub>4</sub>)

Christian Gurtner and Michael J. Sailor\*

Department of Chemistry and Biochemistry, University of California, San Diego,  
La Jolla, California 92093-0358

A. S. Katz and R. C. Dynes\*

Department of Physics, University of California, San Diego, La Jolla, California 92093-0319

Received: October 21, 1997; In Final Form: December 26, 1997

Conducting crystals of the charge-transfer salts TTFBr<sub>x</sub> (tetrathiafulvalenium bromide) and (TMTSF)<sub>2</sub>ClO<sub>4</sub> (bis(tetramethyltetraselenafulvalenium) perchlorate) were studied. The needle-shaped crystals were grown between pairs of platinum or gold electrodes by oxidative electrodeposition. An electrical connection was formed when a crystal growing from one electrode (base electrode) encountered the second electrode (target electrode). It was found that electrical contacts form even if the potential of the target electrode is considerably lower than the electrocrystallization potential of the charge-transfer salt. Contacts between crystal and target electrode are surprisingly adherent, as seen in experiments where crystals detach from the base electrode and stick to the target electrode. They can also be disconnected and reconnected reversibly by manipulation of the potential of the base electrode, which results in dissolution and recrystallization of the organic salt in the vicinity of the target electrode.

## Introduction

The ever increasing complexity and miniaturization of electronic devices creates a need for techniques for the formation and manipulation of structures on a very small length scale. There are a number of new strategies to achieve higher resolution, increase design flexibility, and construct three-dimensional structures that complement standard lithographic methods.<sup>1–10</sup>

We have been interested in the formation of microscopic electronic connections using electrochemical deposition techniques. Electroplating of metals is already widely used for the formation of connections in microelectronics. It has been proposed as a means of repairing small breaks in conventional microcircuits<sup>11</sup> or as a method to construct entire circuits through templated<sup>12</sup> or self-directed<sup>13</sup> deposition reactions. Conducting organic polymers have also shown great promise in the construction of electronic devices such as transistors<sup>14–16</sup> and sensors,<sup>17,18</sup> while the dendritic morphology of electrodeposited conducting polymers has been used to construct three-dimensional networks of connections.<sup>19,20</sup>

Recently we reported that electrical connections can be selectively formed by electrocrystallization of the organic charge-transfer salt TTFBr<sub>x</sub> (tetrathiafulvalenium bromide,  $x = 0.74–0.79$ ).<sup>21</sup> Selectivity was achieved by taking advantage of the highly anisotropic growth and dissolution properties of these crystals. TTFBr<sub>x</sub>, like many other conducting organic charge-transfer salts, forms crystals consisting of separate stacks of donors (TTF) and acceptors (Br) (Figure 1a). Electrocrystallization (oxidation) and electrodisolution (reduction) rates are greatest along the stacking axis which gives the crystals a rod-shaped appearance.<sup>22</sup> This property makes these organic charge-transfer salts interesting candidates for structurally well-defined microscopic conducting wires.

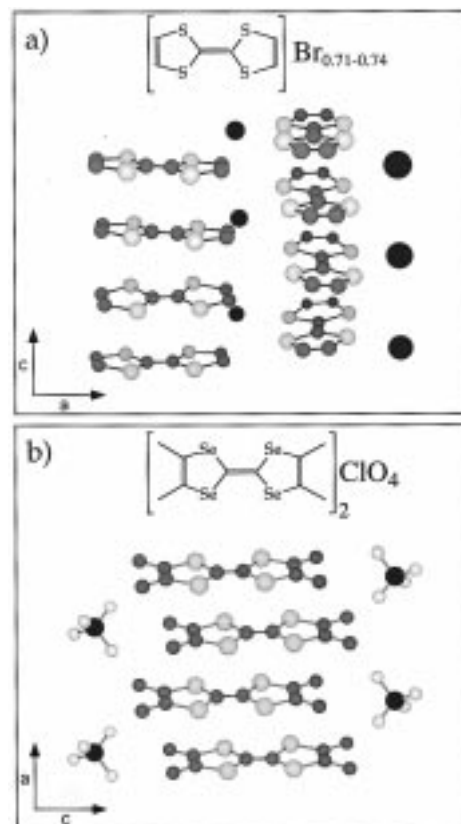


**Figure 1.** (a) Structures of TTFBr<sub>x</sub> ( $x = 0.74–0.79$ ) and (b) (TMTSF)<sub>2</sub>ClO<sub>4</sub>.

In this paper we show that connections built by electrocrystallization of TTFBr<sub>x</sub> and (TMTSF)<sub>2</sub>ClO<sub>4</sub> (bis(tetramethyltetraselenafulvalenium) perchlorate) (Figure 1b) can be reversibly formed and broken electrochemically. We also show that these

\* To whom correspondence should be addressed.

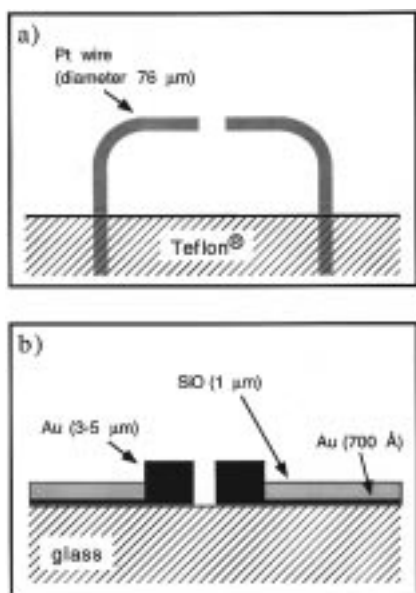


**Figure 2.** Electrode configurations used in the experiments: (a) platinum wire electrodes (diameter  $76\ \mu\text{m}$ ) embedded in Teflon; (b) gold electrodes (thickness  $3\text{--}5\ \mu\text{m}$ , width  $4\text{--}20\ \mu\text{m}$ , depth  $6\ \mu\text{m}$ ) fabricated by using lithography and electroplating.

charge-transfer crystals can form intimate physical contacts when they grow into a metal "target" electrode and under the appropriate conditions can be caused to transfer from one electrode to the other. This behavior has not been observed before and presents interesting possibilities for the formation of three-dimensional conducting structures.

### Experimental Section

Growth of  $\text{TTFBr}_x$  was performed in  $1\text{--}5\ \text{mM}$  solutions of TTF (Aldrich,  $>97\%$ , or Acros,  $>99\%$ ) and  $0.1\ \text{M}$  tetrabutylammonium bromide (Aldrich,  $99\%$ ) in dimethylformamide. Some experiments were performed in acetonitrile and dichloromethane but proved to be less reproducible. Growth of  $(\text{TMTSF})_2\text{ClO}_4$  on lithographed Au electrodes was performed in  $1\text{--}5\ \text{mM}$  solutions of TMTSF (Aldrich,  $97\%$ ) and  $0.01\text{--}0.02\ \text{M}$  tetrabutylammonium perchlorate (Acros,  $99\%$ ) in tetrahydrofuran/heptane (7:3). For the larger Pt electrodes, solutions of  $3\text{--}5\ \text{mM}$  TMTSF and  $0.1\ \text{M}$  tetrabutylammonium perchlorate in THF were used. All solvents were dried and distilled prior to use using standard procedures.<sup>23</sup>

Connections of  $\text{TTFBr}_x$  were grown between pairs of bent Pt wire electrodes (diameter  $76\ \mu\text{m}$ , spacing  $\sim 70\ \mu\text{m}$ ) (Figure 2a) in an airtight two-compartment Teflon cell (8 mL volume). Electrodes were cleaned in concentrated  $\text{HNO}_3$  and rinsed with  $\text{H}_2\text{O}$  and acetone prior to use.

Connections of  $(\text{TMTSF})_2\text{ClO}_4$  were grown between pairs of gold microelectrodes (spacing  $1\text{--}8\ \mu\text{m}$ , thickness  $3\text{--}5\ \mu\text{m}$ ) (Figure 2b) in an airtight two-compartment Teflon cell. The microelectrodes were fabricated by standard photolithography. First, gold leads (thickness  $70\ \text{nm}$ ; resistance ca.  $30\ \Omega$ ;  $5.5\ \text{nm}$  thick chromium underlayer) were thermally evaporated onto a patterned glass substrate and protected by thermal evaporation of a  $1\ \mu\text{m}$  thick insulating layer of  $\text{SiO}_2$ . The microelectrodes were then electroplated on the exposed parts of the leads using a thick film resist. The electrodes were cleaned in dilute  $\text{HNO}_3$  and rinsed with  $\text{H}_2\text{O}$  and acetone prior to use. All experiments were run under potential control with Ag wires or evaporated Ag on glass as quasi-reference electrodes. Potentials were controlled with a PINE AFCBP1 bipotentiostat or two BAS CV-

27 potentiostats. A National Instruments NB-MIO-16 12 bit A/D board on a Macintosh IICI with Igor Pro NIDAQ software (Wavemetrics) was used for data acquisition.

The procedure for growth and trimming of connections has been described elsewhere.<sup>21</sup> In brief, crystals are grown from the base electrode at  $30\text{--}80\ \text{mV}$  positive of the electrocrystallization potential (ECP) while the potential of the target electrode is held at a value at which no observable growth occurs, typically between  $10$  and  $100\ \text{mV}$  negative of the ECP. Nucleation on the base electrode is usually enhanced by an initial potential pulse ( $\sim 1\ \text{s}$ ) to  $100\text{--}150\ \text{mV}$  positive of the ECP. A connection is detected by a sudden flow of current (shunting current) between base and target electrodes.

The dependence of the target electrode potential on the formation of a connection was studied by repetitive growth ( $90\ \text{s}$  at  $+30\ \text{mV}$  relative to the ECP) and dissolution ( $30\ \text{s}$  at  $-20\ \text{mV}$  relative to the ECP) of an individual, connection-forming  $\text{TTFBr}_x$  crystal. In a similar way, the dependence of TTF concentration on the formation and reinforcement of a connection was determined by repetitive growth ( $+30\ \text{mV}$  relative to the ECP, until a shunting current of  $5\ \text{mA}$  was reached) and dissolution ( $-20\ \text{mV}$  relative to the ECP, until the shunting current decayed to  $0.1\ \mu\text{A}$ ) of a connection. The target electrode potential was held at  $-50\ \text{mV}$  relative to the ECP. Slow replacement of the solution through Luer-Lok (Hamilton) ports in the Teflon cell allowed for changes in the TTF concentration without exposing the crystals to excessive mechanical stress caused by turbulence.

Single-crystal conductivities were determined by standard four point probe measurements on  $2\text{--}4\ \text{mm}$  long crystals, grown on  $1\ \text{mm}$  diameter Pt wire electrodes.<sup>24</sup> The crystals were mounted on glass slides, and electrical contacts were made by evaporating  $60\ \text{nm}$  of Au in four separate stripes and attaching  $25\ \mu\text{m}$  diameter Au wires with silver paint (Ted Pella Inc.).

### Results and Discussion

**Formation of Charge-Transfer Salt Connections.** Crystals of most organic charge-transfer salts differ from common metals by exhibiting a large degree of anisotropy in their electrochemical growth and dissolution behavior as well as in their electrical conductivity.<sup>25</sup> Both growth and dissolution processes occur preferentially along the stacking axis of the crystals ( $c$  axis in  $\text{TTFBr}_x$ ,  $a$  axis in  $(\text{TMTSF})_2\text{ClO}_4$ ) (Figure 1). The degree of anisotropy depends on the material studied, but it is very high for both  $\text{TTFBr}_x$  and  $(\text{TMTSF})_2\text{ClO}_4$ . Aspect ratios of up to  $200$  ( $\text{TTFBr}_x$ ) have been observed in our laboratory, but ratios of  $5\text{--}20$  are more commonly observed.<sup>26</sup>  $\text{TTFBr}_x$  crystals have an almost square cross section whereas  $(\text{TMTSF})_2\text{ClO}_4$  crystals have a more rectangular cross section, with typical  $b:c$  axis ratios of  $5:1$ . Both materials display well-defined, smooth, low index crystal faces perpendicular to the stacking axis of the crystals.<sup>22,26</sup>

In our previous work,  $\text{TTFBr}_x$  crystals were electrochemically grown from two separate Pt working electrodes, and a contact was formed when two crystals grew into each other.<sup>21</sup> This method allowed for formation of a connection between electrodes that were spaced more than  $200\ \mu\text{m}$  apart. However, the probability of formation of a successful contact in a reasonably short time was very low. This study focuses on the reversibility and dynamics of connection formation using organic charge-transfer salts. For this purpose, crystals were electrochemically grown from one electrode (the base electrode) while the other electrode (the target electrode) was held at a potential negative of the potential required to induce nucleation. Elec-

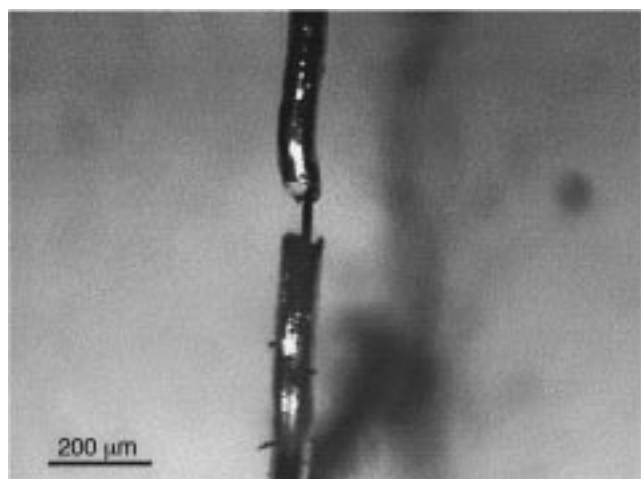


**Figure 3.** Optical photograph of a  $\text{TTFBr}_x$  connection after electrochemical removal of unconnected crystals. Conductance of the connection is 2.5 mS.

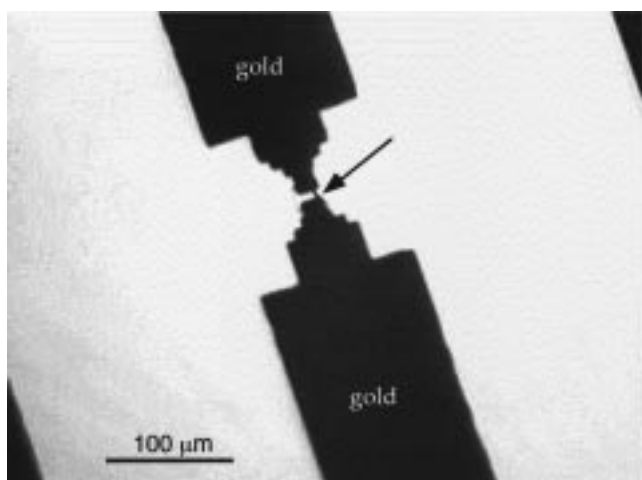


**Figure 4.** Optical photograph of a  $(\text{TMTSF})_2\text{ClO}_4$  connection grown between two Au electrodes. Conductance of the connection is 1.1 mS.

trode geometries were arranged to improve the probability of connection. Two different electrode configurations were used as depicted in Figure 2. In both cases the electrodes were positioned facing each other. The base electrode to target electrode separation was 1–8  $\mu\text{m}$  for the lithographed gold configuration and approximately 70  $\mu\text{m}$  for the platinum wire electrode configuration. The base and target electrodes were connected to a conventional bipotentiostat as independent working electrodes. Connections were fabricated by inducing electrocrystallization of  $\text{TTFBr}_x$  or  $(\text{TMTSF})_2\text{ClO}_4$  at the base electrode. The potential of the base electrode was held several millivolts positive of the electrocrystallization potential (ECP) in order to sustain an appreciable growth rate. A connection was formed when one of the crystals growing from the base electrode contacted the target electrode (Figures 3 and 4 show representative micrographs). The formation of a connection was detected as a sudden jump in current (shunting current) monitored at the target electrode. The shunting current was converted to a conductance value by dividing the value of the current by the potential difference between the base and target electrodes. Typical conductance transients for the formation of  $\text{TTFBr}_x$  and  $(\text{TMTSF})_2\text{ClO}_4$  connections between pairs of Pt wires are shown in Figure 5. Each experiment generates a different conductance transient depending on the geometry and size of the bridging crystal and the morphology of the crystal/

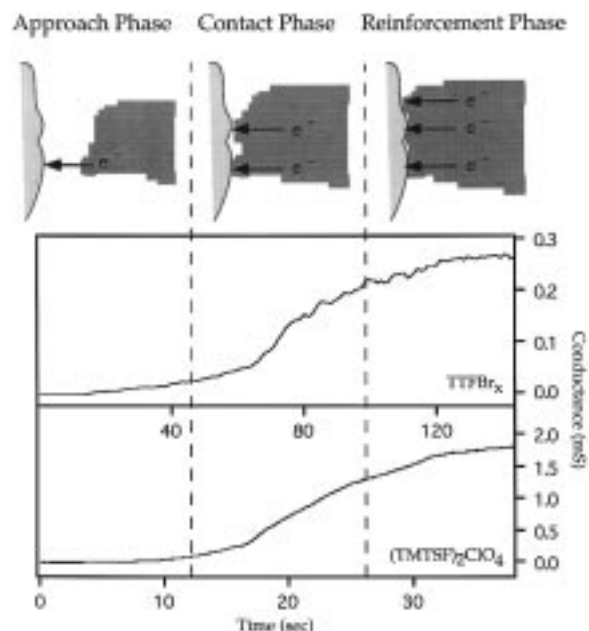


**Figure 5.** Typical conductance traces for  $\text{TTFBr}_x$  and  $(\text{TMTSF})_2\text{ClO}_4$  connections showing the sigmoidal shape indicative for the proposed three phases of connection formation.

metal interface. Despite these differences, most conductance transients had a similar sigmoidal appearance. We interpret the conductance transients in terms of three characteristic formation stages: an “approach phase”, a “contact phase”, and a “reinforcement phase”.

In the “approach phase” (Figure 5) the crystal approaches the target electrode surface by continuous oxidative electrochemical growth at its tip. The decreasing crystal-to-target electrode separation results in the observed increase in conductance, which probably arises from a combination of electrochemical thin film and tunneling currents. The relative contribution from the two currents is expected to vary for different crystal–electrode separations and should depend on the potential of the target electrode, as well as on the solubility of the electrooxidized species. The initial increase in current with decreasing crystal–target electrode separation is analogous to the current increase observed on approach of an SECM (scanning electrochemical microscope) tip to a conducting substrate.<sup>27</sup> However, extraction of distance information using SECM theory is not feasible in our experiments because of the unpredictable dynamic changes in tip geometry and growth rate of the crystal. Thus, there was no obvious correlation between the current transients and target electrode potential. Changes in current due to variations in crystal and electrode geometry probably overwhelm any effects that may arise from thin film or tunneling phenomena.

In the “contact phase” of connection growth a physical interface forms between the crystal and the target electrode. The contact area between the two materials increases until, in extreme cases, it includes the entire cross section of the crystal tip. This growth phase is characterized by a rapid increase in the measured conductance. Contacts at this stage of growth are fragile and easily disrupted; the connection can be readily turned “on” and “off” by small excursions in potential (see below).

In the “reinforcement phase” of connection growth the conductance continues to increase at a constant rate, although in some cases the conductance becomes constant or even decreases (see below). The observation for most of the

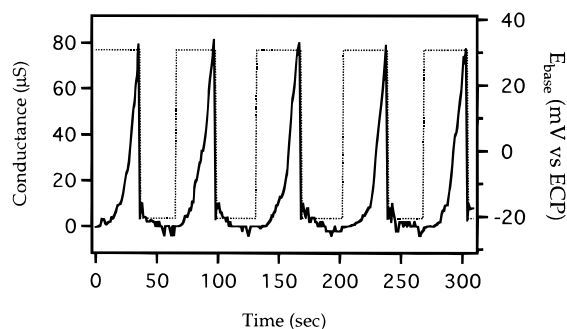


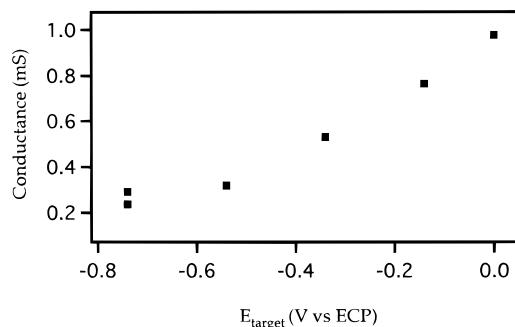
**Figure 6.** Conductance transient (solid line) and potential of the base electrode (dashed line) for a single TTFBr<sub>x</sub> connection during a number of dissolution and reconnection cycles. A full cycle involves a growth period of 90 s at 30 mV positive of the ECP and a dissolution period of 30 s at 20 mV negative of the ECP.

connections, in which the conductance slowly increases with time, is interpreted as a slow increase of the crystal/electrode contact area as the crystal increases in thickness. Since growth of crystals perpendicular to the stacking axis (corresponding to a thickening of the crystal) is a slow process,<sup>26</sup> the increase in conductance is also expected to be slow.

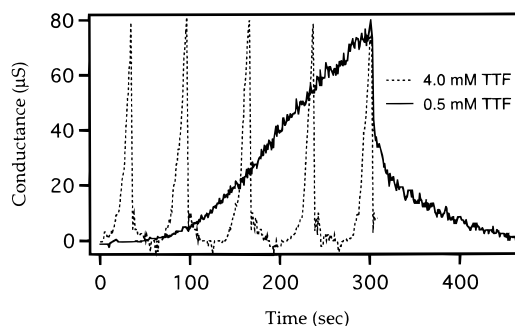
**Reversible Dissolution and Formation of Connections.** A useful feature of many conducting organic charge-transfer salts is the reversibility of the electrocrystallization reaction. Thus, crystals of these materials can be redissolved by electrochemical reduction. In a typical experiment, a connection was established and reinforced under standard conditions until the shunting current reached a predetermined value or until a predetermined period of time had passed. Disconnection was then achieved by reducing the potential of the base electrode to 20 mV negative of the electrocrystallization potential.

Figure 6 shows the conductance transients observed during a series of formation and dissolution cycles for an individual TTFBr<sub>x</sub> crystal connection. As can be seen, the conductance transients for an individual connection are reproducible for many cycles. Some connections were cycled up to 30 times. The number of connect/disconnect cycles obtained was usually limited by other crystals that grew from the base electrode. Over time these additional crystals interfered with the measurements by forming their own connections with the target electrode. The additional crystals can be trimmed while they are still unconnected using a technique developed previously.<sup>21</sup> This allows the system to undergo many more connection/disconnection cycles. The time required to form a connection with a given conductance was found to depend mainly on the potential applied to the base electrode, although the donor and acceptor molecule concentrations, as well as the potential of the target electrode, also have an influence (as discussed below). The rate of crystal dissolution is a function of both the base and the target electrode potentials.<sup>21</sup>

**Influence of the Target Electrode Potential on Connection Formation.** To study the influence of the target electrode potential on the formation of connections between charge-transfer salts and metal electrodes, a single-crystal connection was repeatedly grown and dissolved, and the potential of the target electrode was changed at the beginning of each growth period. Figure 7 shows a plot of the conductance of a typical TTFBr<sub>x</sub> crystal connection as a function of the potential at which the target electrode was held during the growth period. After measurement of the conductance the connection was broken by lowering the potential of the base electrode to 20 mV negative of the ECP, and the connection process was repeated with a new target electrode potential. Connections could be formed



**Figure 7.** Conductance of a TTFBr<sub>x</sub> connection as a function of the potential at which the target electrode was held during a series of 90 s growth periods (experimental conditions are the same as in Figure 6). The two data points for  $E_{\text{target}} = -0.74$  V are taken after the first and last growth period, respectively.



**Figure 8.** Effect of solution concentration of TTF on the conductance transients for a TTFBr<sub>x</sub> connection during dissolution and reconnection cycles.

even when the potential of the target electrode was up to several hundred millivolts negative of the ECP, although the conductance of the connections formed was lowest at these extreme potentials. This is understandable because the potential along the connecting crystal drops according to Ohm's law. Especially at the initial stages of contact, most of the potential drop will occur at the interface between the target electrode and the crystal, decreasing the rate of crystal growth at the tip. Therefore, the connections grown with target electrode potentials most negative of the ECP will have the lowest conductances because their contact areas are smallest. It is also possible that the potential of the target electrode affects the electronic quality of the crystal/electrode contact. The present experiments cannot differentiate between these two possibilities.

**Crystal/Electrode Interfaces.** The efficiency of TTFBr<sub>x</sub> connection formation and reinforcement is affected by the concentration of TTF in solution, as shown in Figure 8. The time required for formation of connections with equivalent conductance is approximately inversely proportional to the solution concentration of TTF. These data are consistent with the assumption that the rate of connection formation is dependent on diffusion of dissolved donor molecules to the tip of the growing crystal. It is unclear to what extent the size of the gap between crystal and target electrode is reduced during crystal growth. The surface roughness of both the crystal tip<sup>26</sup> and the electrode make it appear unlikely that a continuously smooth interface can be formed between the two materials. Furthermore, the influence of the potential of the target electrode is expected to slow down or even prevent crystal growth at very small crystal/electrode separations.

Due to the configuration of the experiment, it is very difficult to obtain conclusive information about either of the metal/crystal interfaces involved in a connection. Room-temperature cur-

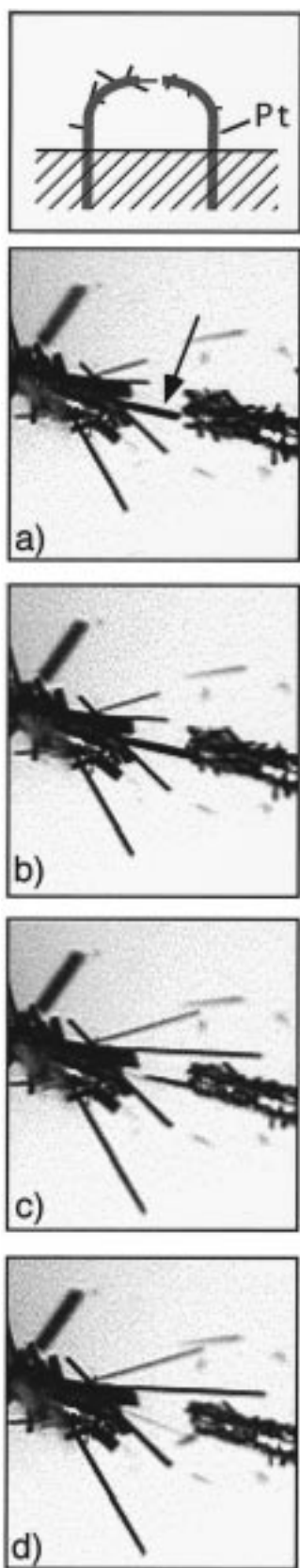


**Figure 9.** Photos showing the “walking” crystal behavior. The sequence of photos with top views of a pair of bent platinum electrodes depicts a  $\text{TTFBr}_x$  crystal (a) growing from the base electrode (b) into the target electrode and then (c) adhering to the target electrode while dissolving away from the base electrode (d) until it breaks off and falls to the bottom of the cell.

rent–voltage measurements in solution and in air indicate that the interface at both electrode contacts is Ohmic, consistent with

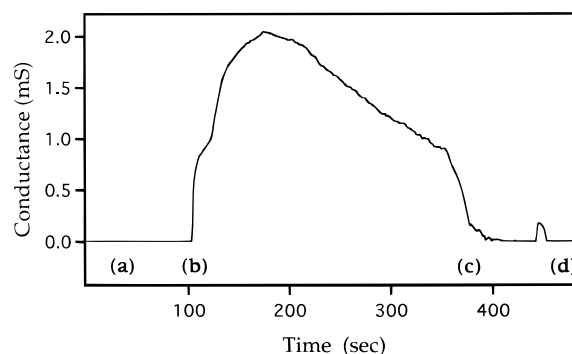


**Figure 10.** Conductance transient for the  $\text{TTFBr}_x$  connection in Figure 9. Potentials of the base and target electrode are +40 mV and –20 mV (vs ECP), respectively.

conductance studies on single crystals of  $\text{TTFBr}_x$  and  $(\text{TMTSF})_2\text{ClO}_4$  with evaporated gold contacts performed in our laboratory and elsewhere.<sup>28,29</sup>

In general, electrodeposited crystals form a less intimate interface with the target electrode than with the base electrode. This is indicated by the response of the crystal to small (<50 mV) changes in applied potential. Even if the target electrode potential is held above the ECP throughout the connection-forming step, the crystal will dissolve from its tip (at the crystal/target electrode interface) when the potential of the base electrode is held below the ECP for extended periods of time. By contrast, adjusting the potential of the target electrode negative of the ECP induces dissolution at the base electrode only occasionally (see below). In most experiments, lowering the target electrode potential by 20–50 mV does not result in a noticeable change in crystal size or connection conductance. This behavior is consistent with the picture of a crystal that is either weakly adhering to the target electrode or separated from it by a less conductive layer (possibly a few monolayers of nonoxidized TTF or a thin solution layer).

Conductances observed after reinforcement of the connections were usually between 5 and 0.5 mS, 1–2 orders of magnitude smaller than would be expected for the measured sizes and conductivities of the crystals. Cross-sectional areas were 1–12  $\mu\text{m}^2$  for crystals grown on Au electrodes and 100 to 900  $\mu\text{m}^2$  for crystals grown on Pt electrodes. Four point probe conductivity measurements on macroscopic crystals grown under our standard conditions gave values of 100–300 S/cm for  $\text{TTFBr}_x$  and 200–600 S/cm for  $(\text{TMTSF})_2\text{ClO}_4$ , in agreement with the literature values for slowly grown single crystals of these materials.<sup>30,31</sup> The reduced conductance for bridging crystals is clearly a sign that at least one of the crystal/metal interfaces possesses a substantial contact resistance.

**“Walking” Crystals.** A different, unpredicted behavior was occasionally observed in the course of connection experiments with  $\text{TTFBr}_x$  where the target electrode potential was held below the ECP. At some point after formation of the connection the conductance gradually decreased until no shunting current was detected. The connecting crystal was then observed to be dissolving away from the base electrode while adhering to the target electrode. This occurred even though the potential on the base electrode was well above the ECP, and the crystal was not expected to dissolve. A typical example of this “walking crystal” behavior is shown in Figure 9. The sequence of images depicts a crystal growing from the base electrode into the target electrode and then adhering to the target electrode while dissolving away from the base electrode. The corresponding conductance transient is shown in Figure 10.

The images in Figure 9 prove that, at least under some circumstances, the crystal forms an adherent connection with the target electrode. The adherence is usually weak (as seen in Figure 9d where the crystal eventually falls off the target electrode) but can often be improved if the potential of the target electrode is stepped above the ECP immediately after the crystal starts dissolving away from the base electrode. In this way the crystal can be regrown and the connection formed again.

The fact that crystals sometimes dissolve at their base instead of dissolving at their tip to display the "walking" behavior is intriguing but not fully understood at this time. A reasonable explanation can be proposed if one assumes that almost all of the potential drop across the connection occurs at the base electrode/crystal contact. This could occur if, for instance, the cross-sectional area of the crystal near the base electrode is very small and therefore the resistance very large. The potential of the entire crystal would then be negative of the ECP, and consequently, the thin crystal base would dissolve, leading to the observed "walking" crystal behavior. A similar effect causes the loss of structural and electrical connectivity in dendritic and fractal metal electrodeposits during electrodisolution.<sup>32</sup> Attempts to purposely induce the "walking crystal" behavior by minor adjustment of various experimental conditions were largely unsuccessful. However, "walking" behavior could be regularly observed if rapid, uncontrolled crystal growth was induced on the base electrode ( $E_{\text{base}} > \text{ECP}$ ) during dissolution of previously grown crystals on the target electrode ( $E_{\text{target}} \ll \text{ECP}$ ). The electrochemical dissolution of crystals from the target electrode creates a high local concentration of donor molecules between the two electrodes, and the rapid crystal growth at the base electrode presumably results in poorly contacted crystals.

**Removal of Crystal Connections from Solution.** Charge-transfer salt connections grown between pairs of Pt wires can be removed from solution with preservation of conductance, although they are susceptible to breakage while the solvent is evaporating due to mechanical stress caused by turbulence and capillary forces. Removal of the smaller connections of (TMTSF)<sub>2</sub>ClO<sub>4</sub> grown between lithographed gold electrodes requires extreme care. (TMTSF)<sub>2</sub>ClO<sub>4</sub> has a finite solubility in most organic solvents usable for electrochemistry, posing an additional problem. In our experience a 7:3 mixture of THF/heptane allowed for electrocrystallization and did not cause noticeable dissolution at open circuit. Nevertheless, only a small number of connections could be recovered from solution even though the cell was flushed at very low flow rates and solvent mixtures were allowed to evaporate slowly. A possible solution to this problem could be removal of the solvents by critical point drying in CO<sub>2</sub>, as has been demonstrated for biological structures<sup>33</sup> or more recently for fabrication of scanning probe cantilevers.<sup>34</sup>

## Conclusions

We have demonstrated that the conducting organic charge-transfer salts TTFBr<sub>x</sub> and (TMTSF)<sub>2</sub>ClO<sub>4</sub> can be used for the reversible formation of electrical connections using electrocrystallization and electrodisolution reactions. The crystal connections have sizes in the low micrometer range. Established contacts between the charge-transfer salts and the electrode materials Pt and Au are Ohmic but show considerable resistance, presumably due to poor interfacial contacts. Connections can be formed relatively independent of the potential of the target electrode. However, the conductance of a connection correlates with the applied potential at the target electrode during growth.

At least in some cases crystals form physically adherent contacts with the target electrode as shown by the observed "walking" crystal behavior. Removal of small connections from solution has proven to be difficult. Therefore, mechanical stability of the connections and procedures for solution removal need to be improved if the materials are to be useful for nanofabricated connections. In addition, the nature of conduction across the crystal/metal interfaces is not known in detail and needs to be further investigated.

**Acknowledgment.** The authors wish to thank the National Science Foundation Young Investigator Award for funding and Professor Paul K. L. Yu and Robert B. Welstand for experimental assistance and helpful discussions. This work was supported by the National Science Foundation, Grant #DMR-9357415, and The Air Force Office of Science and Research, Grant #F4962-092-J0070.

## References and Notes

- (1) Nyffenegger, R. M.; Penner, R. M. *Chem. Rev. (Washington, D.C.)* **1997**, 97, 1195.
- (2) Wu, C.-G.; Bein, T. *Science* **1994**, 264, 1757.
- (3) Martin, C. R. *Science* **1994**, 266, 1961.
- (4) Martin, C. R. *Acc. Chem. Res.* **1995**, 28, 61–68.
- (5) Routkevitch, D.; Bigioni, T.; Moskovits, M.; Xu, J. M. *J. Phys. Chem.* **1996**, 100, 14037.
- (6) Lehmann, O.; Stuke, M. *Science* **1995**, 270, 1644–1646.
- (7) Biebuyck, H. A.; Larsen, N. B.; Delamarche, E.; Michel, B. *IBM J. Res. Dev.* **1997**, 41, 159.
- (8) Kim, E.; Whitesides, G. *Chem. Mater.* **1995**, 7, 1257–1264.
- (9) Whitesides, G. M.; Mathias, J. P.; Seto, C. T. *Science* **1991**, 254, 1312.
- (10) Smela, E.; Inganaes, O.; Lundstrom, I. *Science* **1995**, 268, 1735–1738.
- (11) Gutfeld, R. J. v.; Vigliotti, D. R. *Appl. Phys. Lett.* **1990**, 56, 2584–2586.
- (12) McHardy, J.; Townsend, C. W.; Higley, R.; Ludwig, F. A. Hughes Aircraft Co., U.S. Patent, 5315162, 1994.
- (13) Bradley, J. C.; Chen, H. M.; Crawford, J.; Eckert, J.; Ernazarova, K.; Kurzeja, T.; Lin, M. D.; McGee, M.; Nadler, W.; Stephens, S. G. *Nature* **1997**, 389, 268.
- (14) Kranz, C.; Ludwig, M.; Gaub, H. E.; Schuhmann, W. *Adv. Mater.* **1995**, 7, 568.
- (15) Burroughes, J. H.; Jones, C. A.; Friend, R. H. *Nature* **1988**, 335, 137–141.
- (16) Thackeray, J. W.; Wrighton, M. S. *J. Phys. Chem.* **1986**, 90, 6674–6679.
- (17) Hatfield, J. V.; Neaves, P.; Hicks, P. J.; Persaud, K.; Travers, P. *Sens. Actuat. B* **1994**, 18–19, 221–228.
- (18) Freund, M. S.; Lewis, N. S. *Proc. Natl. Acad. Sci. U.S.A.* **1995**, 92, 2652–2656.
- (19) Curtis, C. L.; Ritchie, J. E.; Sailor, M. J. *Science* **1993**, 262, 2014.
- (20) Sailor, M. J.; Curtis, C. L. *Adv. Mater.* **1994**, 6, 688–692.
- (21) Gurtner, C.; Sailor, M. J. *Adv. Mater.* **1996**, 8, 897–899.
- (22) Carter, P. W.; Hillier, A. C.; Ward, M. D. *J. Am. Chem. Soc.* **1994**, 116, 944–953.
- (23) Shriver, D. F.; Drezdron, M. A. *The Manipulation of Air-Sensitive Compounds*; 2nd ed.; John Wiley and Sons: New York, 1986; pp 84–96.
- (24) Sze, S. M. *Physics of Semiconductor Devices*; John Wiley & Sons: New York, 1981; pp 30–32.
- (25) Ward, M. D. *Electrochemical Aspects of Low-Dimensional Molecular Solids*. In *Electroanalytical Chemistry*; Bard, A. J., Ed.; Marcel Dekker: New York, 1989; Vol. 16, p 181.
- (26) Hillier, A. C.; Ward, M. D. *Science* **1994**, 263, 1261.
- (27) Bard, A. J.; Denuault, G.; Lee, C.; Mandler, D.; Wipf, D. O. *Acc. Chem. Res.* **1990**, 23, 357–362.
- (28) Latif, S. M.; Kroemer, H. *Phys. Rev. B* **1981**, 23, 1887–1895.
- (29) Bechgaard, K.; Jerome, D. *Phys. Scr.* **1991**, T39, 37.
- (30) Bechgaard, K.; Carneiro, K.; Olsen, M.; Rasmussen, F. B.; Jacobsen, C. S. *Phys. Rev. Lett.* **1981**, 46, 852–855.
- (31) Engler, E. M. *Chemtech* **1976**, 274–279.
- (32) Fleury, V.; Barkey, D. *Physica A* **1996**, 233, 730–741.
- (33) Cohen, A. L. *Scanning Electron Microsc.* **1979**, 2, 303–324.
- (34) Stowe, T. D.; Yasumura, K.; Kenny, T. W.; Botkin, D.; Wago, K.; Rugar, D. *Appl. Phys. Lett.* **1997**, 71, 288.